

Nuclear structure of ^{216}Ra at high spin

S MURALITHAR^{1,*}, G RODRIGUES¹, R P SINGH¹, R K BHOWMIK^{1,3},
P MUKHERJEE^{2,†}, B SETHI^{2,†} and I MUKHERJEE²

¹Inter University Accelerator Centre, Aruna Asaf Ali Marg, New Delhi 110 067, India

²Saha Institute of Nuclear Physics, 1/AF Bidhannagar, Kolkata 700 064, India

³Department of Pure and Applied Physics, Guru Ghasidas University, Bilaspur 495 009, India

*Corresponding author. E-mail: smuralithar@gmail.com

MS received 31 July 2011; revised 4 April 2012; accepted 18 April 2012

Abstract. High-spin states of ^{216}Ra ($Z = 88$, $N = 128$) have been investigated through $^{209}\text{Bi}(^{10}\text{B}, 3n)$ reaction at an incident beam energy of 55 MeV and $^{209}\text{Bi}(^{11}\text{B}, 4n)$ reaction at incident beam energies ranging from 65 to 78 MeV. Based on $\gamma\gamma$ coincidence data, the level scheme for ^{216}Ra has been considerably extended up to $\sim 33\hbar$ spin and 7.2 MeV excitation energy in the present experiment with placement of 28 new γ -transitions over what has been reported earlier. Tentative spin-parity assignments are done for the newly proposed levels on the basis of the DCO ratios corresponding to strong gates. Empirical shell model calculations were carried out to provide an understanding of the underlying nuclear structure.

Keywords. HPGe; measured E_γ ; I_γ ; directional correlations from oriented states; lifetime; nuclear structure; γ -ray spectroscopy; empirical shell model.

PACS Nos 21.60.Cs; 21.10.–k; 21.10.Tg; 29.30.Kv

1. Introduction

The shell model concept of effective two-nucleon interactions has been successful in describing properties of ‘magic’ nuclei [1]. Nuclear structure of nuclei around ^{208}Pb ($Z = 82$, $N = 126$) in low-spin region, can be understood in terms of effective interactions. However, nuclear structure at high spin and excitation energies (~ 6 MeV) would require a coupling of excited $1p-1h$ with ^{208}Pb core. The coupling between single-particle orbitals and collective vibrations of core complicates the simple shell model picture. With increasing neutron number, Ra isotopes show an abrupt change from individual particle model to collective model from ^{217}Ra to ^{218}Ra . It would be interesting to investigate the collective behaviour at high spins in Ra isotopes in this region.

[†]Deceased

The presence of approximately similar number of valence protons (N_p) and neutrons (N_n) leads to reflection asymmetry or octupole instability. In ^{216}Ra , number of valence particles ($N_p = 6$ and $N_n = 2$) is too few to show collective behaviour for the nucleus. The coupling to octupole 3^- state in ^{208}Pb may give rise to enhanced collectivity in high-spin states. The strongly interacting proton–neutron combinations leading to isomeric states in these nuclei facilitate experimental and theoretical investigations. Octupole vibration coupling to multiparticles in valence orbitals $\pi(h_{9/2}, f_{7/2}, i_{13/2})$ and $\nu(g_{9/2}, i_{11/2}, j_{15/2})$ leads to octupole deformation and configuration of mixed isomers with enhanced characteristic $E3$ decays [2] in this mass region. The $E3$ transitions are allowed single-particle transitions for both protons and neutrons, viz., $\pi i_{13/2} \rightarrow \pi f_{7/2}$ and $\nu j_{15/2} \rightarrow \nu g_{9/2}$. The strong attractive nucleon–nucleon interaction is important for high-spin states on and near the yrast line, as it significantly lowers excitation energy of those levels with aligned high- j components. The maximum spin that may be attributable to such an aligned configuration in ^{216}Ra , would be of the order of $J \sim 39 \hbar$ with a wave function of $\pi(h_{9/2}^2 f_{7/2}^2 i_{13/2}^2)_{26^+} \otimes \nu(i_{11/2} j_{15/2})_{13^-}$. At such high spins, core excitation will compete with alignment of valence particles.

The stretched two-neutron high-spin states in ^{210}Pb have been studied [3] from the reaction $^{208}\text{Pb}(\alpha, ^2\text{He})$ at 55 MeV incident energy. Six proton states are known [4] for ^{214}Ra . It will be of great interest to study high-spin states of ^{216}Ra and correlate them with coupled states of ^{210}Pb and ^{214}Ra . Although ^{216}Ra was studied by several groups [4–10] earlier, only levels up to 23^- state at 4976 keV are firmly established in these works. Above 13^- state, a sudden branching to several close lying levels hampered construction of decay scheme towards higher excitation and spin. The aim of the present work is to explore the level scheme, nature of high-spin states and the isomeric decays in ^{216}Ra .

2. Experiment

The experiment was done using heavy ion beams from the 15 UD Pelletron accelerator [11] at Inter University Accelerator Centre and γ 's were recorded with Gamma Detector Array (GDA) [12] consisting of 12 Compton suppressed HPGe ($\sim 25\%$ relative efficiency) detectors and a multiplicity filter of 14 BGO detectors. A systematic study of ^{216}Ra was done using two reactions: (1) $^{209}\text{Bi}(^{10}\text{B}, 3n)$ at 55 MeV and (2) $^{209}\text{Bi}(^{11}\text{B}, 4n)$ at 65, 70, 78 MeV incident beam energies. The beam was pulsed at 4 MHz. The pulsed beam helped in measuring the lifetime of nuclear levels between the beam pulses as the lifetime of isomers were of the order of 10 ns only. The ^{209}Bi target of 3.5 mg/cm^2 thickness was made by using a rolling mill. Typical beam current of 1 pA was applied on the target. The CAMAC-based data acquisition system, 'FREEDOM' [13], was used to collect data in list mode and it required at least two suppressed Ge detectors in coincidence. The data were collected with energy, time from all Ge detectors, hit pattern from Ge, time from beam pulser and multiplicity from 14 BGO detectors when there was $\gamma\gamma$ coincidence. Around 1.8×10^8 , two and higher fold events were recorded. The list mode data were analysed to create coincidence spectra using the program 'NSCSORT' [14]. The γ -rays belonging to various nuclei were identified by putting gates on known strong transitions, which were assigned to respective nuclei by earlier workers. The γ 's from fusion evaporation channels dominated as fission cross-sections are lower in the above reaction.

Dividing relative time spectrum between γ 's into three regions (before – 150 ns, prompt – 30 ns and after – 150 ns) enabled categorization of coincident γ -rays based on their arrival time with respect to gating transition. If a nucleus has an isomer with lifetime comparable to electronic resolving time (~ 10 ns) then 'before-prompt-after' relations can be established which help in ordering partial cascades of transitions.

Good quality $\gamma\gamma$ coincidence data were obtained from four Compton-suppressed Ge detectors, at angles 45° , 99° and 153° with respect to beam direction, in the GDA facility. The timing signals from all Ge detectors were recorded in 16-channel TDC in common start $\gamma\gamma$ mode. In off-line analysis, time spectrum (TAC) between any two γ 's for each event could be generated based on time difference of the corresponding detectors. In off-line analysis, data were sorted to produce $E_\gamma-E_\gamma$ $4\text{k} \otimes 4\text{k}$ matrices, with 0.5 keV per channel gain, as given below:

- (1) Each detector vs. rest of the detectors
- (2) With time condition using TAC as 'early' or 'late' (within 150 ns) coincidences
- (3) With time condition using TAC as 'prompt' (within 30 ns) coincidences
- (4) Forward detectors (45°) vs. detectors at 99° and backward detectors (153°) vs. detectors at 99°

In addition to these matrices, γ -gated $\gamma\Delta T$ matrices were generated for getting time spectrum between any two γ 's of ^{216}Ra which enabled lifetime measurement of isomeric nuclear levels.

3. Results and discussion

The construction of level scheme was facilitated by the presence of isomers which allowed partial γ -ray cascades. The intensities of coincident γ -rays were used as constraints to remove ambiguities in level ordering. We took advantage of the fact that in spectra projected from a given gating transition, intensities of transitions originating from higher lying states follow singles intensities, whereas γ -rays lying below gating transitions are reduced relative to their singles intensities, as side-feeding to lower levels is not observed in coincident spectrum. In addition, when absolute γ -ray coincidence intensities are measured, cascades lying below gating transition should all have the same intensity when internal electron conversion fraction is taken into account.

The singles and coincidence γ -spectra are shown in figure 1 which was used in getting relative intensities of γ 's in ^{216}Ra . The $\gamma\gamma$ coincidence spectra in 'prompt' and 'before' time window are given in figures 2 and 3 respectively. From these two spectra, one could identify the γ -cascades below and above the isomers, respectively. This is further confirmed using time spectrum between coincident γ 's. The time spectrum was constructed between any two coincident γ 's of ^{216}Ra to ascertain the presence of isomers. The timing from all detectors were matched properly by calibrating all channels of TDC. The time spectra generated for typical prompt and delayed coincidence from ^{216}Ra are given in figure 4. We measured lifetime of the isomer using these data.

Using angle-dependent $E_\gamma-E_\gamma$ $4\text{k} \times 4\text{k}$ matrices we inferred the type of multipolarity of γ -transition by directional correlations from oriented states (DCO) method [15]. By gating on a known transition in a nucleus, angle-gated spectra can be obtained from which

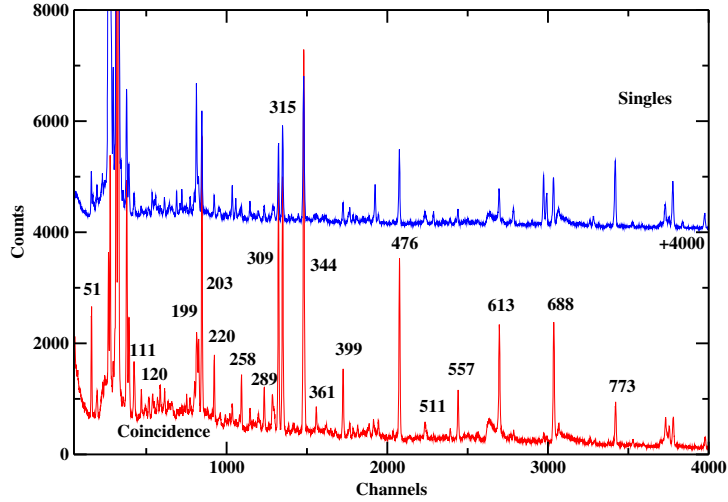


Figure 1. The singles and $\gamma\gamma$ coincidence spectra from fusion evaporation reaction $^{209}\text{Bi}(^{11}\text{B}, 4n)$.

intensity anisotropy of the emitted γ was obtained. We define the intensity anisotropy, R_{DCO} as

$$R_{\text{DCO}}(\gamma_1) = \frac{I(\gamma_1) \text{ at } 99^\circ \text{ gated by } \gamma_2 \text{ at } 153^\circ}{I(\gamma_1) \text{ at } 153^\circ \text{ gated by } \gamma_2 \text{ at } 99^\circ}, \quad (1)$$

where stretched $\Delta J = 1$ and $\Delta J = 2$ are expected to have values 2.0 and 1.0 respectively. Assuming commonly encountered situation of stretched transition, when we gate on a

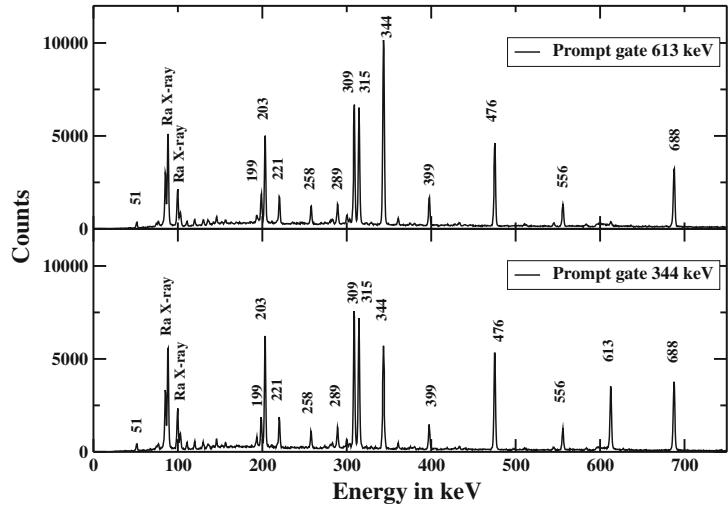


Figure 2. The γ -ray spectrum obtained from 'prompt' coincidence time window (50 ns) for transitions in ^{216}Ra .

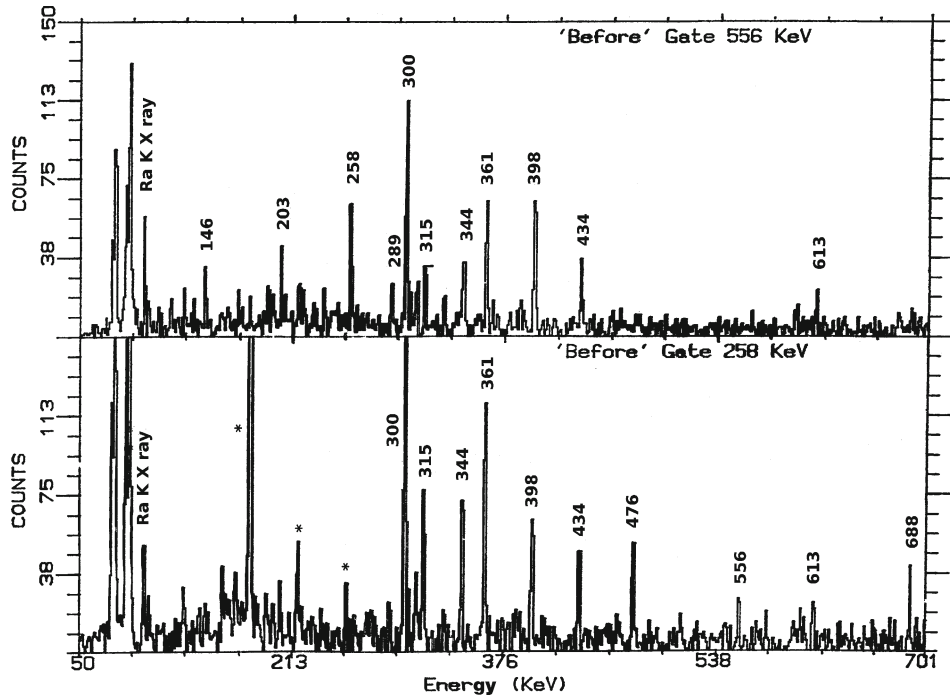


Figure 3. The coincidence spectrum from ‘before’ time window (150 ns) which has enhanced intensity for γ -transitions above the isomers. The γ ’s marked with (*) are contaminant lines from ^{214}Ra populated simultaneously in the same reaction along with ^{216}Ra .

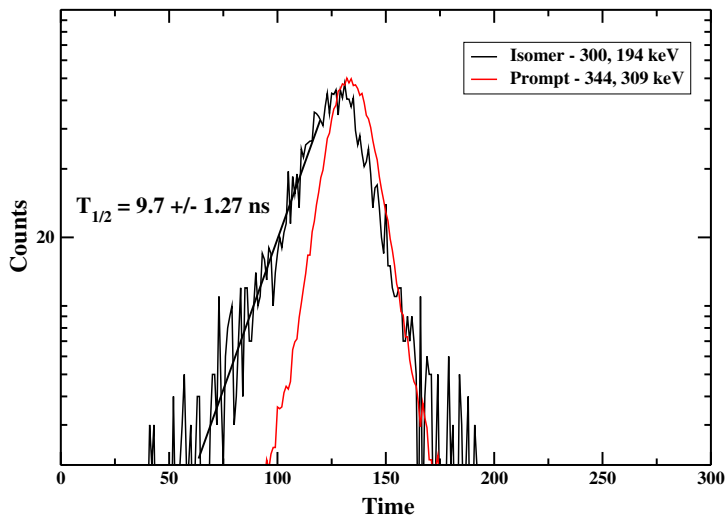


Figure 4. The time spectra gated by coincident γ ’s confirming 9.7 ± 1.2 ns as the lifetime of isomer for the level excitation energy of 5.546 MeV and spin $27\hbar$ in ^{216}Ra .

quadrupole ($\Delta J = 2$) transition, all quadrupole transitions would have similar intensities in both the gated spectra (spectrum at 153° with gate at 99° and vice versa), whereas the intensity of dipole transitions would differ by a factor of two in both spectra. All in-band $\Delta J = 1$ transitions are assigned as $E1$ or $M1$, while $J = 2$ transitions are assigned as $E2$. The results of this procedure on experimental data using gate on quadrupole and dipole transitions in ^{216}Ra is shown in figure 5. The measured relative intensity and DCO ratio of γ 's are given in table 1. The rest of the γ 's placed in level scheme have intensity less than 5% due to which DCO ratios could not be measured for them. It may be noted that the intensity balance across levels could only approximately be done due to large internal conversion of some of the low energy γ -transitions.

The level scheme of ^{216}Ra developed from this experimental data is shown in figure 6. This is based on excitation function, relative intensity, DCO ratio and $\gamma\gamma$ coincidence relationship. The energy levels up to 19^- agree well with the schemes suggested by the earlier workers. The notable addition to level scheme is the extension of yrast sequence up to $\sim 33\hbar$ spin and 7.2 MeV excitation energy in the present experiment with placement of 28 new γ -transitions compared to the work in [5]. The data collected enabled us to measure DCO ratios of 194, 300, 361 and 434 keV which helped to remove ambiguities in the spin of nuclear levels up to $J = 31\hbar$. Earlier reported [5], 132 and 168 keV transitions were not observed in our data. The time conditions helped to establish several new transitions above 8.7 ns isomeric level at 3764 keV. In contrast to ref. [8] ordering of 613 and 344 keV γ -transitions were interchanged based on relative population of these levels at two bombarding energies. This ordering of γ 's agrees with ref. [16] which was also based on the intensity of γ 's from excitation function.

In $\gamma\gamma$ coincidence spectra, γ -transitions below 200 keV are rather weak as internal conversion process dominates and timing from Ge is poor compared to high-energy γ .

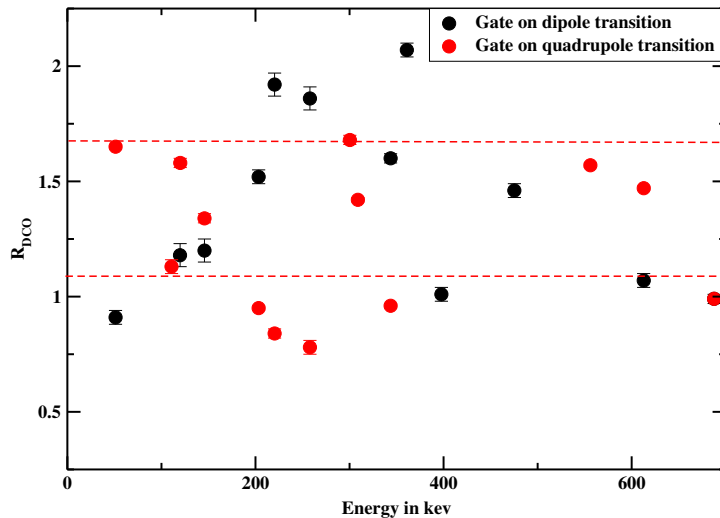


Figure 5. DCO ratios for γ -transitions in coincidence with 315 keV, quadrupole transition and 556 keV, dipole transition of ^{216}Ra . The horizontal dashed straight lines indicate average values for two different types of γ -transitions.

Nuclear structure of ^{216}Ra at high spin

Table 1. Transition energy (E_γ), relative intensity (I_γ), DCO ratios (R_{DCO}), l of gating γ , nature of transition and decay from an initial state (J_i^π) to the final state (J_f^π) for transitions placed in level scheme of ^{216}Ra are listed.

E_γ (keV)	I_γ in % (Rel.)	R_{DCO} γ	l of Gating γ	Type of transition D or Q	$J_i^\pi \rightarrow J_f^\pi$
52.0	30.7(0.7)	0.91(0.03)	D	D	$19^- \rightarrow 18^+$
111	9.3(1.3)	1.13(0.03)	D	D	$20^- \rightarrow 19^-$
120	6.4(1.9)	1.58(0.02)	Q	D	$21 \rightarrow 20^-$
130	6.6(1.8)	1.04(0.03)	Q	Q	$18^+ \rightarrow 16^+$
137	<5				
147	6.7(1.2)	1.2(0.03)	D	D	$23 \rightarrow 22$
152	<5				
157	<5				
170	<5				
194	9.2(1.9)	1.7(0.04)	Q	D	$27 \rightarrow 26$
199	20.2(1.6)	1.91(0.04)	D	Q	$18^+ \rightarrow 16^+$
200	<5				
203.5	75.0(1.1)	0.95(0.02)	Q	Q	$8^+ \rightarrow 6^+$
217	<5				
221	14.7(0.4)	1.92(0.05)	D	Q	$16^+ \rightarrow 14^+$
228	<5				
248	<5				
258	15.1(0.8)	1.86(0.05)	D	Q	$26 \rightarrow 24$
274	<5				
282	<5				
289	15.1(0.7)	1.67(0.06)	D	Q	$16^+ \rightarrow 14^+$
300	15.7(0.6)	1.68(0.02)	Q	D	$28 \rightarrow 27$
304	<5				
309	94.5(0.9)	1.42(0.01)	Q	D	$11^- \rightarrow 10^+$
315	97.4(0.8)	1.82(0.01)	D	Q	$10^+ \rightarrow 8^+$
323	<5				
329	<5				
335	<5				
343.5 doublet	188.2(0.7)	0.96(0.02)	Q	Q	$6^+ \rightarrow 4^+$
344 doublet			Q	Q	$13^- \rightarrow 11^-$
361	9.1(1.3)	2.07(0.03)	D	Q	$30 \rightarrow 28$
398	32.8(0.8)	1.01(0.03)	D	D	$24 \rightarrow 23$
418	<5				
423	<5				
433	<5				
434	6.8(1.9)	1.21(0.05)	D	D	$31 \rightarrow 30$
476	95.9(0.5)	1.01(0.03)	Q	Q	$4^+ \rightarrow 2^+$
546	<5				

Table 1. *Continued.*

E_γ (keV)	I_γ in % (Rel.)	R_{DCO} γ	l of Gating γ	Type of transition D or Q	$J_i^\pi \rightarrow J_f^\pi$
556	33.5(0.9)	1.01(0.02)	D	D	$22 \rightarrow 21$
584	<5				
613	93.2(0.6)	1.07(0.03)	D	D	$14^+ \rightarrow 13^-$
628	<5				
688	100	0.99(0.02)	Q	Q	$2^+ \rightarrow 0^+$
744	<5				
763	<5				
934	<5				
1002	<5				
1088	<5				

The relative placement of levels, where low-energy γ -transitions are involved, can only be confirmed by studying the reaction with an electron spectrometer along with Ge array.

The order of 199 and 220 keV γ -transitions are reversed in the level scheme compared to [5] as per the intensities of γ 's in the data. Even though the placement of 289 keV γ is the same as in Itoh *et al*, the 130 keV γ is placed above the nuclear excitation level with spin $27\hbar$ as the transition is too weak and coincidence with other γ 's justifies the placement. The 120 keV γ is placed below $21\hbar$ while it was placed above $14^+\hbar$ in [5]. The new found 147 keV γ is placed between the levels with spins $23\hbar$ and $22\hbar$, while Itoh *et al* did not report this transition because the detectors they employed in the experiment was less efficient. The better sensitivity of γ -array allowed us to find new 329, 217, and 763 keV γ 's and they are placed above $30\hbar$ as per the intensity and coincidence information extracted from data.

4. Shell model calculations

The pioneering work of using effective two-body interactions in shell model theory was done by deShalit and Talmi [1]. As ^{208}Pb formed a remarkably inert core, the concept was applied successfully by Blomqvist *et al* [17] to nuclei in the Pb region. Using empirical two-nucleon matrix elements rather than the theoretical ones, significant success was achieved for a few nucleon cases. In this work, we calculate empirically the excitation energies for ^{216}Ra in terms of six proton states from ^{214}Ra [4] coupled with two neutron states from ^{210}Pb [3], i.e., added energies of the levels from ^{214}Ra and ^{210}Pb whose spin make up to total spin in ^{216}Ra and gives the excitation energy close to the experimental excitation energies for that nuclear level. The excitation energies of zeroth order for levels of ^{216}Ra in terms of coupled stretched states for these two nuclei are compared with data from this experiment and are given in table 2 and figure 7.

The shell model configurations of a majority of newly observed high-spin states in ^{216}Ra were obtained by this procedure. The fit of the calculated excitation energies by

Nuclear structure of ^{216}Ra at high spin

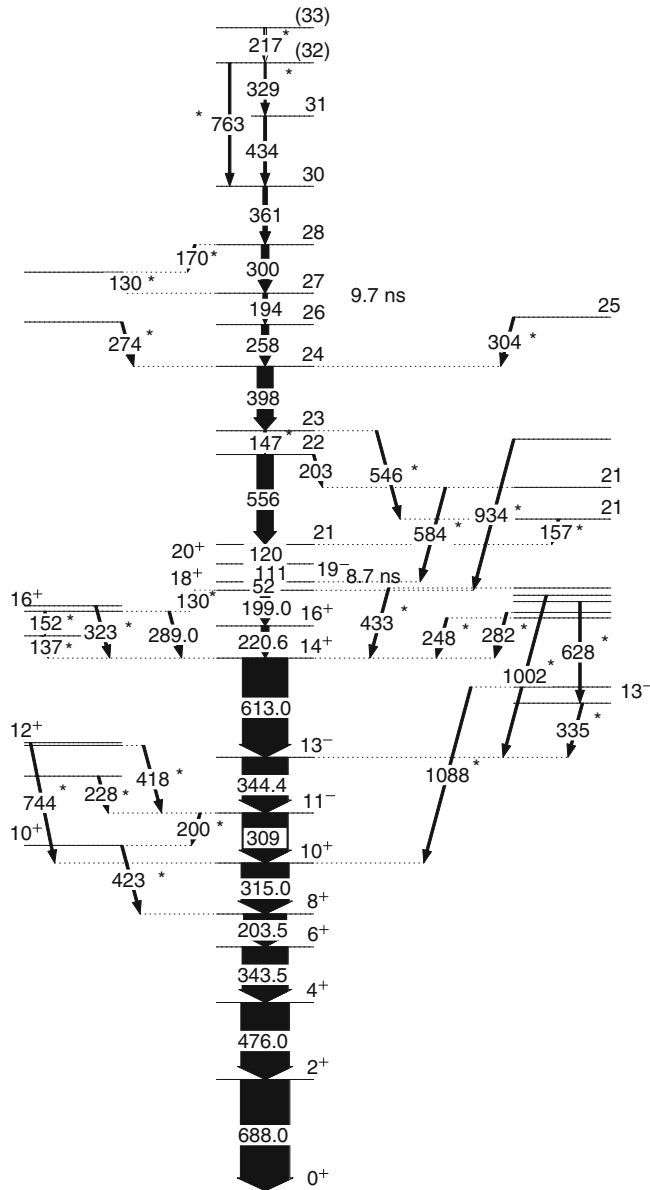


Figure 6. The level scheme of ^{216}Ra as obtained in the present work. The lifetimes of isomers are marked in ns along with spin. The newly placed γ -transitions are marked with (*).

empirical shell model (ESM) with the level energies obtained in this experiment is presented in figure 8. The residual interaction amongst valence particles with two neutrons and six protons in valence space is not affecting the excitation energy of levels up to 5.4 MeV excitation energy. This can be noticed from the fact that energy difference between ESM excitation energies and experimental level energies is less than 0.5 MeV

Table 2. The comparison of level energies of ^{216}Ra measured in the present work and calculated excitation energies by empirical shell model (ESM).

Level spin (\hbar)	^{210}Pb spin (\hbar)	^{210}Pb energy (MeV)	^{214}Ra spin (\hbar)	^{214}Ra energy (MeV)	ESM ^{216}Ra energy (MeV)	Expt. ^{216}Ra energy (MeV)
2 ⁺	2 ⁺	0.80	0 ⁺	0	0.80	0.69
4 ⁺	4 ⁺	1.10	0 ⁺	0	1.10	1.16
6 ⁺	6 ⁺	1.20	0 ⁺	0	1.20	1.50
8 ⁺	8 ⁺	1.21	0 ⁺	0	1.21	1.71
10 ⁺	10 ⁺	1.80	0 ⁺	0	1.80	2.03
11 ⁻	11 ⁻	2.52	0 ⁺	0	2.52	2.34
12 ⁺	8 ⁺	1.21	4 ⁺	1.64	2.85	2.77
13 ⁻	13 ⁻	3.13	0 ⁺	0	3.13	3.01
14 ⁺	6 ⁺	1.20	8 ⁺	1.87	3.07	3.29
16 ⁺	8 ⁺	1.21	8 ₁ ⁺	1.87	3.08	3.51
16 ⁺	8 ⁺	1.21	8 ₂ ⁺	2.07	3.28	3.58
18 ⁺	10 ⁺	1.80	8 ₂ ⁺	1.87	3.67	3.71
19 ⁻	8 ⁺	1.21	11 ⁻	2.68	3.89	3.76
20 ⁺	8 ⁺	1.21	12 ⁺	3.26	4.47	3.88
21 ⁻	10 ⁺	1.80	11 ⁻	2.68	4.48	4
22 ⁺	8 ⁺	1.21	14 ⁺	3.48	4.69	4.55
23 ⁻	8 ⁺	1.20	15 ⁻	3.99	5.20	4.70
24 ⁺	10 ⁺	1.80	14 ⁺	3.48	5.28	5.10
25 ⁻	8 ⁺	1.21	17 ⁻	4.15	5.36	5.40
26 ⁺	10 ⁺	1.80	16 ⁺	4.24	6.04	5.35
28 ⁺	8 ⁺	1.21	20 ⁺	5.24	6.45	5.85
30 ⁺	10 ⁺	1.80	20 ⁺	5.24	7.04	6.21
31 ⁻	10 ⁺	1.80	21 ⁻	5.39	7.19	6.64

up to $I^\pi = 25^-$. The residual interaction comes into play only when nuclear excitation energy is comparable to nucleon separation energy ($S_n = 7$ MeV).

The shell model calculations for ^{216}Ra using all the available orbitals for valence particles is unwieldy with the available computing resources. The shell model calculation with Nushell [18] was carried out with khp interaction, $jj67pn$ model space and restricting maximum valence particles occupation to six protons in $1h_{9/2}$ and maximum two neutrons in the orbitals $i_{11/2}$, $g_{9/2}$, $g_{7/2}$, $d_{5/2}$, $d_{3/2}$, $s_{1/2}$, $j_{15/2}$. Even though spin sequences observed in experimental data were reproduced by Nushell calculation, excitation energies were less by a factor of two with respect to experimental figures due to severe truncation of the model space.

ESM energy values are useful because they indicate essential nature of the structure of wave function and limitations of this method of calculation. Deviations of ESM indicate that states in ^{216}Ra are in reality not just two non-interacting neutrons coupled to ^{214}Ra states. The number of protons and the neutrons is eight and are interestingly not interacting with each other even after coming together in ^{216}Ra . The agreement between ESM and experimental values in low-spin region ($J < 20^+$) indicates that the nn and np interactions are not strong enough to disturb the overall agreement observed. The neutron

Nuclear structure of ^{216}Ra at high spin

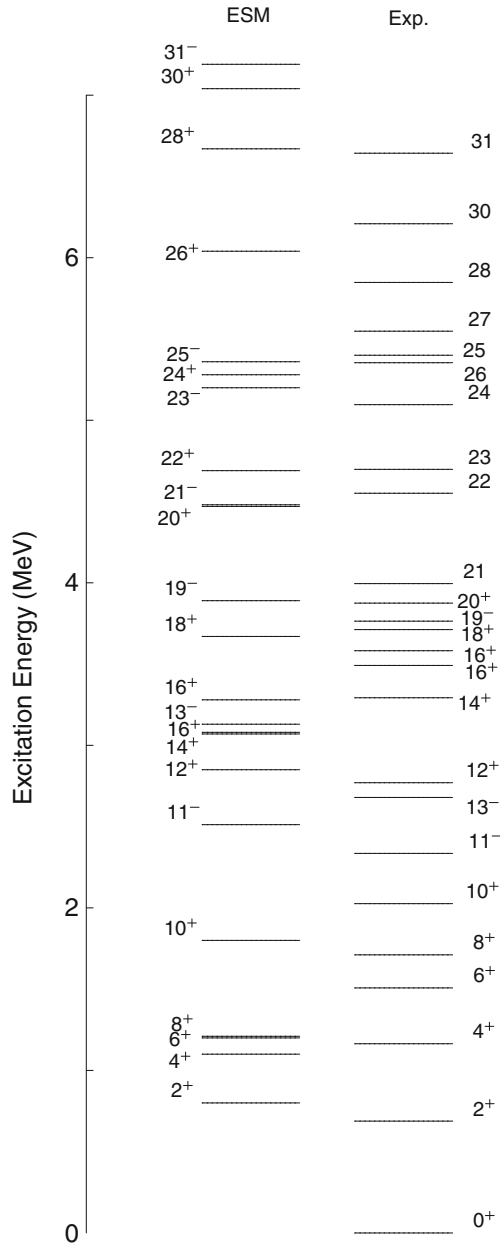


Figure 7. The excitation energies of high-spin states of ^{216}Ra obtained from this experiment (Exp.) are compared with theoretical values calculated by the empirical shell model (ESM).

multiplets contribute to excitation energies in the low-spin region while proton excitation contributes to excitation energies in higher-spin region. The deviation between ESM and experimental values in high-spin region ($J > 20^+$) indicate that the nn and np interactions

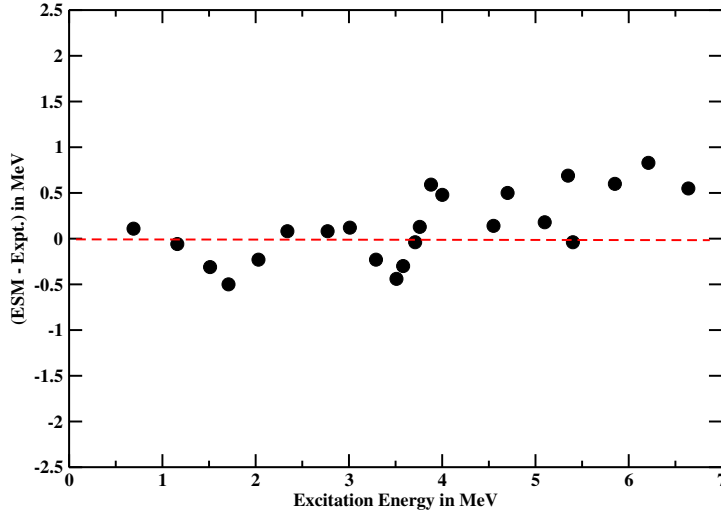


Figure 8. The difference between excitation energy calculated by empirical shell model (ESM) and level energy of high-spin states of ^{216}Ra obtained from this experiment (Exp.) is plotted against experimental level energies.

are not completely zero and contribute to this deviation. At high spin, many combinations of spins from six protons and two neutrons contribute to single state leading to lowering of excitation energy due to configuration mixing of levels. Further, having two neutrons above the neutron magic number 126 in ^{216}Ra opens up the possibility of coupling of neutron and proton excitations which could contribute to many of the high-spin states. The particle-hole excitations also happen at higher excitation energies.

In the high-spin region ($J > 20^+$), the plot of excitation energy vs. $J(J+1)$ shows good linear fit in ^{216}Ra compared to ^{214}Ra [4]. The slope of the above-mentioned plot (gives moment of inertia, i.e. $2 * \mathfrak{I}/h^2$) is $\sim 249 \text{ MeV}^{-1}$ for ^{216}Ra while ^{214}Ra plot has a slope of $(2 * \mathfrak{I}/h^2) \sim 104 \text{ MeV}^{-1}$. It indicates that at higher spins, ^{216}Ra behaves more like a rigid rotor compared to ^{214}Ra . As a result, the ^{216}Ra spectra generated from weak coupling approximation (ESM) start failing strongly at higher spins.

5. Conclusion

High-spin states and isomeric levels in ^{216}Ra were investigated using a γ detector array. The levels were populated up to the excitation energy of 7.2 MeV and $J \sim 33\hbar$ with placement of 28 new γ -transitions over what has been reported earlier. Starting from the known γ -transitions so far observed in $\gamma\gamma$ coincidence experiment, many new transitions were found through coincidences. Tentative assignment of spin-parity of levels was done using measured DCO ratios and relative intensities of transitions. We have identified many new levels feeding the known isomers, with spin 27 and 19^- using tagged time-difference technique. The experimental level energies of ^{216}Ra were compared with the result of empirical shell model-based calculation. The collective nature of the bands in

Nuclear structure of ^{216}Ra at high spin

^{216}Ra could be classified as vibrational from the level scheme obtained and based on systematics of many levels in $A \sim 216$ region.

Acknowledgements

This work was funded by the University Grants Commission. The authors are thankful to Pelletron staff of IUAC for providing excellent pulsed beam during experiments. One of the authors (SM) would like to thank M Sarkar and S Sarkar for valuable discussions on ESM calculations. The authors thank A Roy for fruitful discussions.

References

- [1] A de-Shalit and I Talmi, *Nuclear shell theory* (Academic, New York, 1963)
- [2] A E Stuchbery *et al*, *Nucl. Phys.* **A641**, 401 (1998)
- [3] P Von Neumann-Cosel *et al*, *Phys. Rev.* **C47**, 1027 (1993)
- [4] A E Stuchbery *et al*, *Nucl. Phys.* **A548**, 159 (1992)
- [5] Y Itoh *et al*, *Nucl. Phys.* **A410**, 156 (1983)
- [6] M Schramm *et al*, *Hyperfine Interactions* **59**, 165 (1990)
- [7] M Adachi *et al*, *Nucl. Phys.* **A442**, 361 (1985)
- [8] A Chevallier *et al*, *Z. Phys.* **A308**, 277 (1982)
- [9] T Nomura *et al*, *Phys. Lett.* **B58**, 273 (1975)
- [10] M Sugawara *et al*, *J. Phys. Jpn.* **53**, 2956 (1984)
- [11] G K Mehta and A P Patro, *Nucl. Instrum. Methods* **A268**, 334 (1988)
- [12] S C Pancholi and R K Bhowmik, *Indian J. Pure and Appl. Phys.* **27**, 660 (1989)
- [13] B P Ajith Kumar *et al*, *Proceedings of the Symposium on Advances in Nuclear and Allied Instr.* **51** (1997)
- [14] R K Bhowmik *et al*, *DAE Symp. Nucl. Phys.* **34B**, 419 (1991)
- [15] A Kramer-Flecken *et al*, *Nucl. Instrum. Methods* **A275**, 333 (1989)
- [16] T Lonroth *et al*, *Phys. Rev.* **C27**, 180 (1983)
- [17] Blomqvist *et al*, *Phys. Rev. Lett.* **38**, 534 (1977)
- [18] Nushell @ MSU, B A Brown and W D M Rae (unpublished), <http://www.nscl.msu.edu/brown/>